Spanish Journal of Palaeontology 41 (1), 2026
https://doi.org/10.7203/sjp.33856
Sociedad Española de Paleontología ISSN 2255-0550 / eISSN 2660-9568

OPEN ACCESS RESEARCH PAPER

Inside the head of *Pelecanimimus polyodon* (Ornithomimosauria, Dinosauria): Occipital palaeoneuroanatomy of the early branching ornithomimosaur from Las Hoyas fossil site (Early Cretaceous, Cuenca, Spain)

Dentro de la cabeza de *Pelecanimimus polyodon* (Ornithomimosauria, Dinosauria): Paleoneuroanatomía occipital del ornitomimosaurio basal del yacimiento de Las Hoyas (Cretácico Inferior, Cuenca, España)

Xairo CALVO-PÉREZ & Elena CUESTA

Abstract: Ornithomimosauria is a striking theropod dinosaur group whose unusual traits have generated debate about several behaviours related to diet and lifestyle. Although the palaeoneuroanatomy might provide valuable information to palaeobiological studies of this group, these studies are scarce. Only the endocast of *Struthiomimus* is known, despite several complete skulls having been recovered in this group. In other non-avian maniraptoriforms, palaeoneuroanatomical studies are not overly plentiful either, restricting themselves to well-characterised endocasts within Therizinosauria and Oviraptorosauria. Here, we present the palaeoneuroanatomy of the endocranial cavity of *Pelecanimimus polyodon*, an ornithomimosaur from the Early Cretaceous of Cuenca (Spain). The occipital region of its braincase is studied using CT scans, providing information about the inner ear, the hindbrain, cranial nerves, and vascular tracts. Its endocranial morphology is similar to *Struthiomimus* and follows the evolutionary trends of Coelurosauria. *Pelecanimimus* shows a reduced and posterior dural peak, and elongated semicircular canals; thus, good gaze stabilisation is inferred and strongly agrees with the non-avian to avian brain evolution. The lagena of *Pelecanimimus* is short, so high-frequency values of hearing are inferred for the taxon compared with other non-avian theropods. Those results are expected for an early-branching maniraptoriform, and positively contribute to our knowledge of the evolution of Coelurosauria and Theropoda.

Resumen: Los ornitomimosaurios son un grupo de dinosaurios terópodos con características peculiares que suscitan debate sobre diversos comportamientos. La paleoneuroanatomía esclarecería algunas de estas incógnitas, pero estos estudios son aún muy escasos en el grupo. Solo se conoce el encéfalo de *Struthiomimus,* a pesar de que se han recuperado varios cráneos completos de ornitomimosaurios. En otros maniraptoriformes no avianos, tampoco abundan estos estudios, limitándose a moldes de Therizinosauria y Oviraptorosauria. En este trabajo se estudia la cavidad endocraneana de *Pelecanimimus polyodon*, un ornitomimosaurio del Cretácico Inferior de Cuenca (España). La región occipital de su neurocráneo se analiza usando tomografías computarizadas, reconstruyéndose el oído interno, el rombencéfalo, los nervios craneales y los tractos vasculares. Su morfología es similar a la de *Struthiomimus* y encaja con las tendencias evolutivas en Coelurosauria. *Pelecanimimus* muestra una expansión dorsal reducida y posterior, y canales semicirculares alargados; infiriéndose una buena estabilización de la cabeza, concordando con lo observado hacia el encéfalo aviano. La lagena de *Pelecanimimus* es corta, en comparación con otros terópodos no avianos. Esos resultados son los esperados para un maniraptoriforme basal y contribuyen positivamente a nuestro conocimiento de la evolución de los celurosaurios y los terópodos.

Received: 24 March 2026
Accepted: 24 April 2026
Published: 8 June 2026

Corresponding author:
Xairo Calvo-Pérez
xairocp@gmail.com

Keywords:
Theropoda
Coelurosauria
Barremian
Palaeoneurology
Sensorial capabilities
Encephalon

Palabras-clave:
Theropoda
Coelurosauria
Barremiense
Paleoneurología
Capacidades sensoriales
Encéfalo

INTRODUCTION

The palaeoneuroanatomy studies of Theropoda have been mainly focused on the basal members of the group recently (Lautenschlager *et al.*, 2012), such as ceratosaurs (Sanders & Smith, 2005; Cerroni & Paulina-Carabajal, 2019), megalosauroids (Schade *et al.*, 2020), allosauroids (Paulina-Carabajal & Canale, 2010; Paulina-Carabajal & Currie, 2012; Paulina-Carabajal & Nieto, 2019) or non-maniraptoriform coelurosaurs (Witmer & Ridgely, 2009; McKeown *et al.*, 2020). Nevertheless, some brain cavity studies

have been carried out for several nested clades from Maniraptoriforms, especially for Therizinosauria (Lautenschlager *et al.*, 2012) and Oviraptorosauria (Franzosa, 2004; Kundrát, 2007; Balanoff *et al.*, 2013, 2014, 2018). Those have been especially helpful in understanding the ecological and ethological adaptations of these groups and unravelling the avian brain evolution and the origin of flight in Dinosauria.

Ornithomimosauria represents an early branching clade of Maniraptoriforms, placing it as the sister taxon of Maniraptora. This group of non-avian theropod dinosaurs were widely distributed throughout the world, being especially abundant in Cretaceous beds of Asia and North America (Makovicky *et al.*, 2004). Striking ethological and palaeoenvironmental features have been inferred for ornithomimosaurs, such as herbivorous/omnivorous feeding behaviour (*e.g.,* Barrett, 2005). However, sensory biology studies are scarce in Ornithomimosauria. Only the brain cavity endocast of *Struthiomimus altus* has been reconstructed (Witmer & Ridgely, 2009), but without firm conclusions about its functions. Studies about olfactory acuity analysed this ability in various taxa of the group (*Struthiomimus*, *Ornithomimus*, *Garudimimus*, '*Dromiceiomimus brevitertius*'), but without a detailed description of the encephalic casts (Zelenitsky *et al.*, 2008, 2011). These types of studies are factually more abundant in other coelurosaurs (*e.g.,* tyrannosauroids; Witmer & Ridgely, 2009; Bever *et al.*, 2011; Paulina-Carabajal & Currie, 2017; McKeown *et al.*, 2020), which represents a knowledge gap for the neuroanatomy of Ornithomimosauria.

Pelecanimimus polyodon Pérez-Moreno, Sanz, Buscalioni, Moratalla, Ortega & Rasskin-Gutman, 1994 is a basal ornithomimosaur from the Early Cretaceous of Las Hoyas fossil site (Cuenca, Spain). The holotype includes the anterior half of the skeleton, from the skull to the forelimbs (Pérez-Moreno *et al.*, 1994; Cuesta *et al.*, 2018a, 2021a). Although divided into two halves and slightly deformed, the skull is complete and almost totally articulated (Cuesta *et al.*, 2018a). This fact allows several studies and inferences over the skull of *Pelecanimimus*, involving both sensory and ethological conclusions.

With more than 200 teeth, the herbivorous/omnivorous hypothesis is not as easily supported in *Pelecanimimus* as in more deeply nested, fully edentulous ornithomimosaurs (Barrett, 2005). Nevertheless, those teeth could have acted as a single cutting edge due to their closely packed distribution, similar to a beak or rhamphotheca (Pérez-Moreno *et al.*, 1994), making the herbivorous/omnivorous hypothesis more heavily supported (Zanno & Makovicky, 2011).

The outstanding preservation state of the skull allowed the reconstruction of the scleral ring (Calvo-Pérez *et al.*, 2022, 2023a, 2023b), a structure closely related to the sense of vision. Following the methodology developed by Choiniere *et al.* (2021), several measurements of this bony structure were taken when reconstructed and compared with those of other extinct and extant vertebrates. These procedures allowed to infer that *Pelecanimimus* probably was more active during the night, like other small coelurosaurs, and also to establish nocturnality as a basal feature within Ornithomimosauria (Calvo-Pérez *et al.*, 2023b).

The whole skull of *Pelecanimimus* was scanned by computed tomography (CT scan), so all parts could be segmented, reintegrated, rearticulated and retrodeformed. Both these scanning and reconstruction procedures allowed to describe in detail and almost completely the features of the skull and enabled potential ethological and eco-morphological analyses (Cuesta *et al.*, 2021b). However, the brain anatomy of *Pelecanimimus polyodon* remains ununderstood. Therefore, an endocranial reconstruction is proposed for this species, involving the encephalon, sense organs, neurovascular tracts, and pneumatic cavities. This work will shed light on the way of life of *Pelecanimimus*, allowing to better understand the ethological patterns and ecology of the species. It will help to unravel the feature, sense, and brain evolution in Ornithomimosauria and Maniraptoriforms.

MATERIAL AND METHODS

Material

MUPA-LH 7777 (Museo de Cuenca, Cuenca, Spain) is the holotype of *Pelecanimimus polyodon*. It includes the articulated anterior half of the skeleton, which is composed of the skull, complete cervical vertebra series, all anterior dorsal vertebrae and some posterior ones, ribs, pectoral girdle, sternum, and the two forelimbs (Pérez-Moreno *et al.*, 1994; Cuesta *et al.*, 2018a, 2021a). The slab and counterslab, encompassing the skull and the most anterior cervical vertebrae (Fig. 1), were scanned at the Fukui Prefectural Dinosaur Museum (Katsuyama, Japan), using a TXS320-ACTIS (TESCO Co., Yokohama, Japan) CT scanner with a voltage of 217 kV and a current of 153 µA. The scan of the slab produced 1821 slices, each with an inter-slice gap of 0.1 mm, and an image resolution of 816 x 323 pixels. The scan of the counterslab, on the other hand, yielded 2231 slices with the same 0.1 mm inter-slice spacing and an image resolution of 988 x 354 pixels. Before this work, the complete skull of *Pelecanimimus* had been individually segmented by bone, reconstructed, and retrodeformed, and a detailed osteological description is currently in preparation (Cuesta *et al.*, 2018b, 2021a). The record of the braincase is formed by the two frontals, the parietal and the occipital region. These pieces are isolated from each other, deformed, and not articulated in the fossil. The occipital region is the best-preserved element of the braincase, and, hence, it was used for this study. Future approaches will be made, when the complete skull of *Pelecanimimus* is restored. This region is split in the two slabs of the specimen. This splitting is not perfectly sagittally divided, and

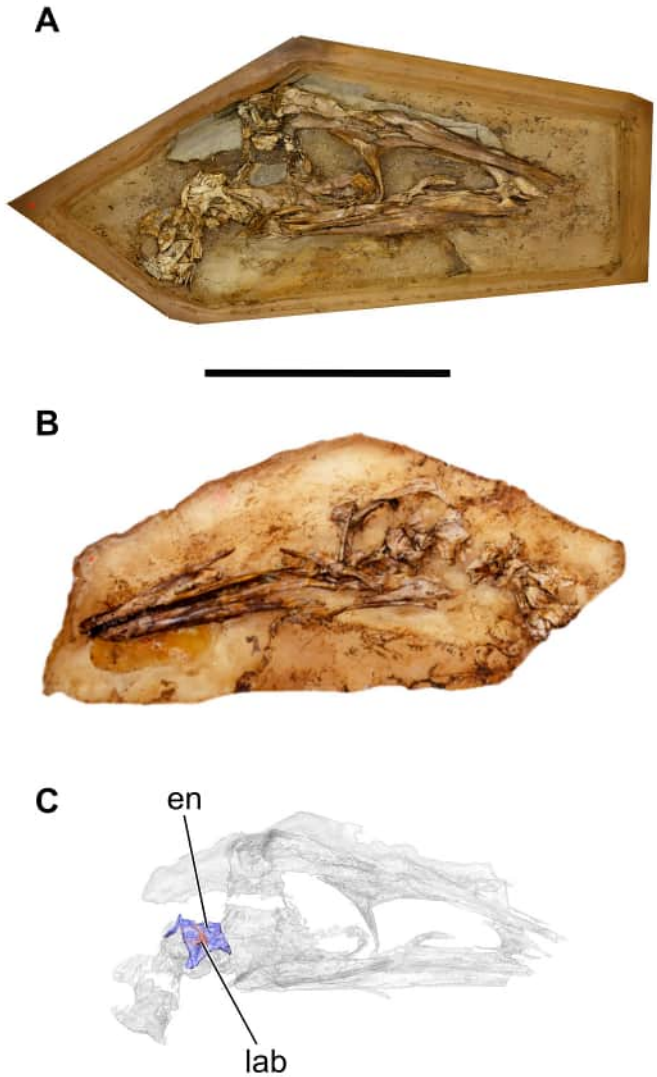

Figure 1. *Pelecanimimus polyodon* holotype MUPA-LH 7777, encompassing the skull and the most anterior cervical vertebrae. **A,** Right lateral view of the right slab; **B,** left lateral view of the left slab; **C,** digital reconstruction of the skull, cranial endocast and inner ear from the right slab in right lateral view; semitransparency is applied to bone to allow observation of internal structures. **Abbreviations: en,** cranial endocast; **lab,** endosseous labyrinth (= inner ear); scale bar = 100 mm.

the cutting area divides the bone diagonally, and most of it is preserved in the right slab. Therefore, in this right slab, there is preserved part of the ventral region of the supraoccipital, right exoccipital-opisthotic complex (with a complete paraoccipital process), most of the basioccipital complex, most of the complete basisphenoid, the right prootic, and the right laterosphenoid. The occipital condyle, the right basal tuber, and the right basipterygoid process are mostly preserved in this slab. The braincase in the left slab is not as well-preserved as the right part. It just preserves some even bones of the lateral wall and part of the odd bones of the occipital region of the braincase: most of the supraoccipital, the left exoccipital-opisthotic complex (including the complete left paraoccipital process), a small region of the basioccipital, and part of the left side of the basisphenoid.

The CT scan of the skull was used to identify, segment, and reconstruct the different structures related to the endocranial cavity, including the cast of the encephalon and sense organs, pneumatic recesses, and nervous and vascular passages. This procedure was improved thanks to the 3D reconstructions of the occipital region of the braincase, which represent a handy resource for checking the accuracy of the position and identifying the new reconstructed structures.

Reconstruction

The endocranial structures of the holotype of *Pelecanimimus polyodon* were segmented using 3D Slicer v.5.6.2. All these structures represent the cast of the cavities where the organs were housed, not knowing the original volume of them. However, in the main text, they are usually specified with the anatomical name of the structure that they represent, not referring to the fact that they are casts to avoid redundancy and repetition.

The complete braincase is lateromedially compressed and deformed. Because of this, frontal and transversal planes would be the most useful for visualizing and processing the CT volume. This fact implied that, in terms of the 3D Slicer, XY and YZ were the main planes for segmentation.

The segmentation was performed by progressively checking the CT volume from the XY and YZ planes, slice by slice, and selecting cavities and hollow areas, both empty or potentially filled with sediment. Posteriorly, those selected materials were studied and individually identified as particular structures. Brightness and contrast adjusting and density range selection were handy resources for differentiating the structures from other cranial materials over the CT volume. The segmented areas were also contrasted with the 3D reconstruction of the occipital region of the braincase. It provided a more accurate selection and identification of the different structures by checking their shape and position over the surface of the skull reconstruction.

For every segmented structure, a 3D model was created. It entailed creating 3D meshes of those materials in 3D Slicer, posteriorly saving each structure as an exportable file. The structures were saved as OBJ files, which are highly compatible files with most 3D software.

The segmented anatomic elements were posteriorly processed using Geomagic Studio 2014 to repair, reconstruct, and retrodeform the mesh to compensate for the compression suffered by the fossil, and then saved as STL files.

Anatomical terminology and colour codes for the CT-based rendering follow those of Witmer and Ridgely (2009).

Measurements

The measurements of the endocranial reconstructed structures were made using MeshLab v.2022.02. Every structure was loaded individually in MeshLab as a new mesh. Then, the measurements were taken using the measuring tool, which allows us to take straight measurements.

For the inner ear, since the structure is curved and more complex, the measurements were obtained using Amira v9.2. The inner ear was skeletonized using the *Auto Skeleton* tool in Amira (Skeletonization), following the methodology proposed by Benson *et al.* (2017). The skeletonization allows us to obtain accurate midline lengths of an image data from the segmentation. This tool extracts, from the segmented image data, the centreline of interconnected regions and converts this *skeleton* to a Spatial Graph object, that consists of nodes and segments. After the skeletonization, landmarks were selected (Fig. 2) from the nodes indicating the different structures of the inner ear of interest (*i.e.,* semicircular canals and lagena), and then, the segments between these landmarks were measured using the *Line Set* tool in Amira.

Hearing calculation

The length of the lagena is commonly used to estimate the hearing sensitivity and auditory capabilities of extinct animals (*e.g.,* Gleich *et al.*, 2005; Walsh *et al.*, 2009; Witmer & Ridgely, 2009; Choiniere *et al.*, 2021). Here, two methodologies have been selected to estimate the relative size of the lagena. The first is based on the ratio between the length of the lagena and the height of the complete labyrinth as a comparison method with other taxa. The second is based in the study of Choiniere *et al.* (2021). It is the calculation of the relative elongation of the lagena (Fig. 3) based on the ratio between its length and the height of the braincase (from the skull roof to the ventral surface of the basisphenoid). Due to the disarticulation of the braincase from the skull, it is challenging to determine the precise height of the braincase of *Pelecanimimus*. Nevertheless, the estimation of the contact between the parietal and supraoccipital is based on previous skull reconstructions (Cuesta *et al.*, 2021b). The height is then measured from this point to the ventral surface of the basisphenoid (Fig. 3). Choiniere *et al.* (2021) established a qualitative classification of the elongation of the lagena in short, limited, moderate and high, using a correlation between these two variables. Furthermore, the qualitative elongation of the lagena was linked to diel activity pattern and foraging behaviour by Choiniere *et al.* (2021), which made it possible to infer these patterns and behaviours in *Pelecanimimus.* The hearing sensitivity of *Pelecanimimus* is calculated based on the studies by Gleich *et al.* (2005). Using a sample of extant birds (Gleich *et al.*, 2005), the frequency of best hearing is predicted within a range of two values. These values are calculated following a regression line obtained from extant taxa. The first value of the range is obtained as a function of the body mass, and the second value as a function of the basilar papilla length. The basilar papilla is estimated as two thirds of the total cochlear duct length (referred here as lagena). The body mass of *Pelecanimimus* was already calculated in Zanno and Makovicky (2013), based on Christiansen and Fariña (2004) equations. Despite the absence of a femur in the holotype of *Pelecanimimus,* the authors estimated its length based on relative skull length (see suppl. in Zanno & Makovicky, 2013). The methodology proposed by Walsh *et al.* (2009) has not been used, since the anteroposteriorly braincase length is unknown in *Pelecanimimus*.

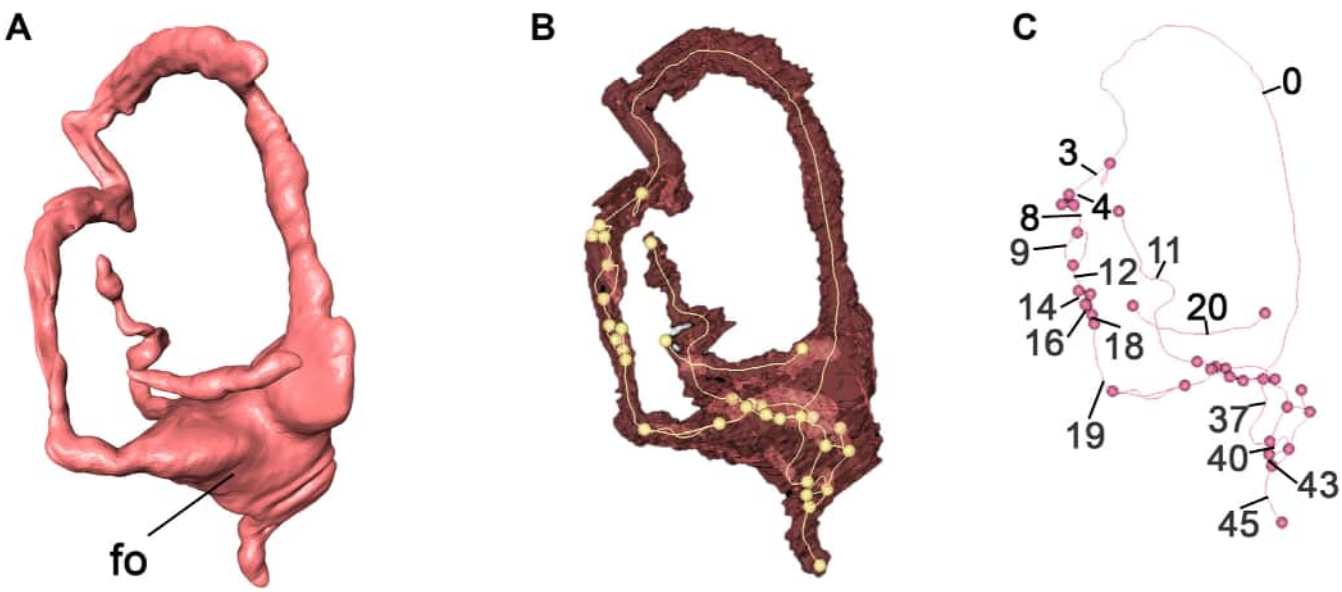

Figure 2. Process of the skeletonization in Amira. **A,** Reconstructed inner ear after segmentation; **B,** inner ear after skeletonising using the *Auto skeletonization* in Amira; **C,** landmarking of the labyrinth and the lines that were used to measure. Numbers indicate the number of the lines that were used for measurements in Table 1. **Abbreviations: fo,** fenestra ovalis.

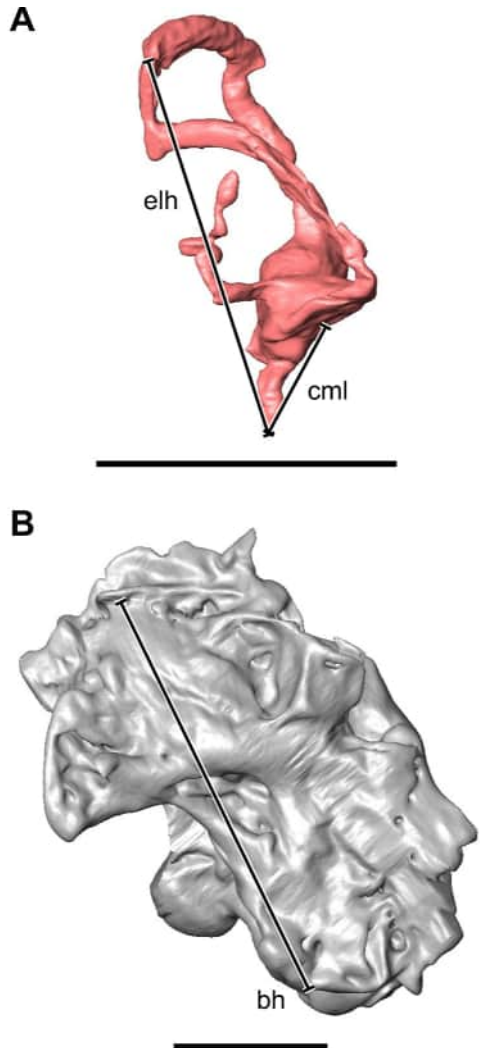

Figure 3. Cochlear duct maximum length, endosseous labyrinth height, and braincase height measurement method. **A,** Anterior view of the right endosseous labyrinth of *Pelecanimimus polyodon* indicating cochlear duct maximum length and endosseous labyrinth height measurements; cochlear duct maximum length is measured from the fenestra ovalis to the ventral tip of the lagena; **B,** right lateral view of the occipital region of the braincase of *Pelecanimimus polyodon* indicating braincase height measurement; methodology by Choiniere *et al.* (2021). **Abbreviations: bh,** braincase height; **cml,** cochlear duct maximum length; **elh,** endosseous labyrinth height; scale bars = 10 mm.

RESULTS

Cranial endocast

The cranial endocast cavity was highly affected by the lateromedial taphonomical compression. Furthermore, the endocranial cavity has been the most affected by the sediment matrix filling; thus, the scan resolution was affected by a low contrast between sediment and bones. Although this was a challenge, most of the occipital cranial endocast was directly segmented from the CT scan, including the medulla oblongata. Afterward, the regions that were unable to be accurately segmented due to the CT scan resolution were reconstructed (Fig. 4).

The anterior part of the midbrain and the whole forebrain, including the cerebral hemispheres, were not possible to segment and reconstruct since most of the bones in the skull roof (*e.g.,* frontal, parietal) and in the lateral wall of the braincase (*e.g.,* orbitosphenoid, laterosphenoid) are disarticulated, deformed or missing (see above). A more comprehensive segmentation and reconstruction of the entire endocast of *Pelecanimimus* will be feasible through future 3D reconstruction and retrodeformation of the complete skull. The entire hindbrain was possible to be segmented. Posteriorly, the cerebellum area was mainly restored and retrodeformed since it was the area where the taphonomical compression affected the most to the braincase. As seen in other ornithomimosaurs (Witmer *et al.*, 1997; Makovicky & Norell, 1998; Hattori *et al.*, 2023), a marked, dorsoventrally expanded dorsal tympanic recess is excavated in the lateral wall of this area of the braincase, on the prootic-opisthotic region (Fig. 5A, 5C). Internally, the braincase preserved the otic cavity (Fig. 5E), including the medial wall, well-preserved (see below). The medial wall is inflated medially, forming the vestibular eminence. In this cavity, there is a slightly wide recess that could be the floccular recess (Fig. 5E). This recess continues excavating through the medial wall of the otic cavity and opens internally on the last one. The flocculus is identifiable following the recess (Fig. 4). The reconstructed flocculus is short. However, due to the lateromedial compression of the skull, the complete length of the flocculus might have been affected.

Although the medulla oblongata was segmented entirely, it is filled with sediment in the fossil, so the morphology could not precisely reflect the original anatomical form. The preserved and reconstructed part of the cranial endocast is 21.8 mm long. Dorsally, the endocast preserves part of the dural peak (= pyramidal peak or pineal peak; Witmer & Ridgely, 2009) that is positioned posterior to the cerebral hemisphere, just dorsal to the inner ear (Fig. 4A–4B). This arrangement resembles to that in other coelurosaurs as *Struthiomimus* or *Deinonychus* (see Witmer & Ridgely, 2009). However, the dural peak of *Pelecanimimus* is located posterior to the position observed in non-maniraptoriform coelurosaurs, such as *Tyrannosaurus* (Witmer & Ridgely, 2009) and *Daspletosaurus* (Paulina-Carabajal *et al.*, 2021). And it is, even, more posterior to the position seen in *Murusraptor* (Paulina-Carabajal & Currie, 2017) or non-coelurosaurian theropods, such as the abelisauroids *Majungasaurus* (Witmer & Ridgely, 2009) and *Carnotaurus* (Cerroni & Paulina-Carabajal, 2019), or the allosauroids *Giganotosaurus* (Paulina-Carabajal & Nieto, 2019), *Acrocanthosaurus* (Franzosa & Rowe, 2005) and *Allosaurus* (Witmer & Ridgely, 2009). This dural peak is reduced, similar to *Struthiomimus* and distinct from the elevated peaks in early branching averostra such as *Viavenator*, *Majungasaurus* or *Allosaurus* (*e.g.,* Witmer & Ridgely, 2009; Paulina-Carabajal & Filippi, 2018). The dural peak is at the level of the prootic and, thus, it may be

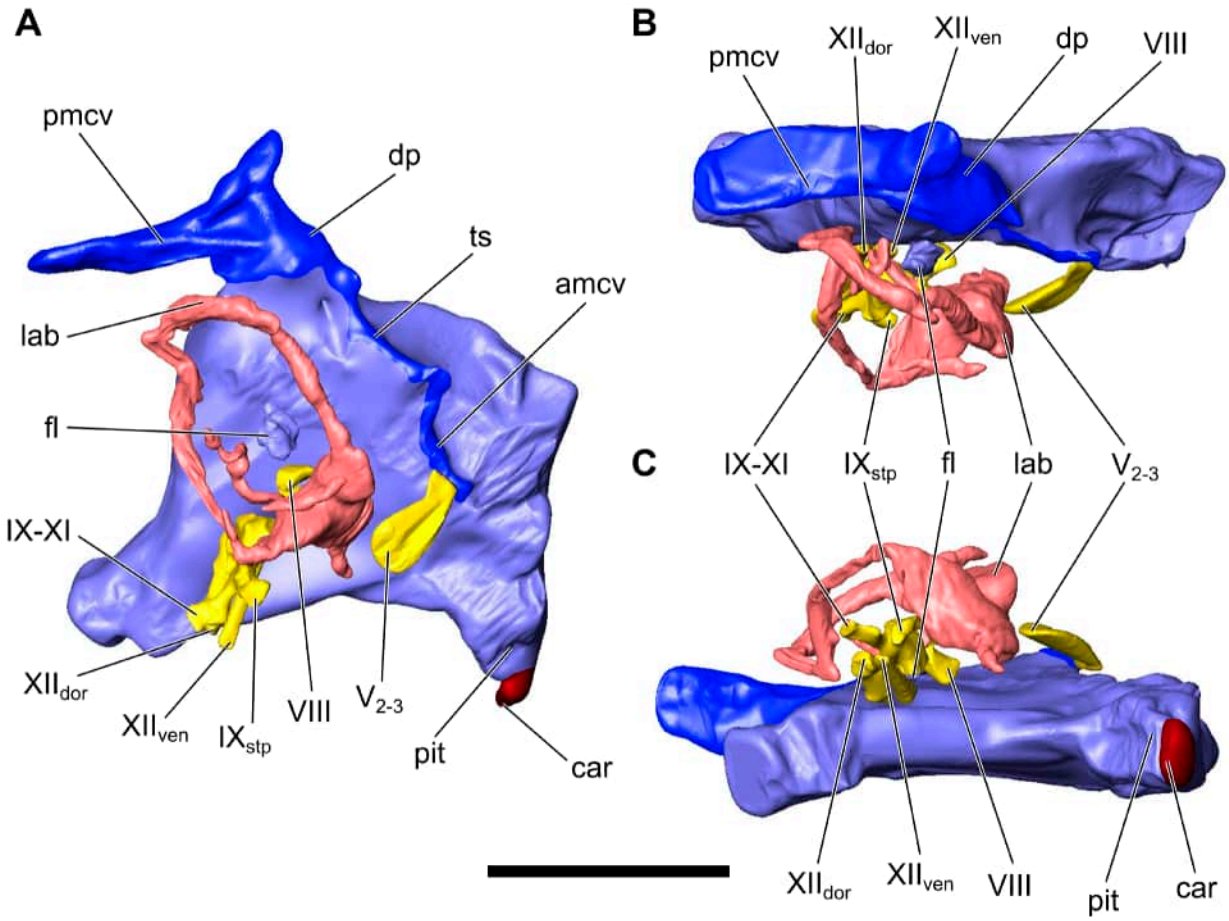

Figure 4. Digital reconstruction of the cranial endocast and cast of the inner ear of *Pelecanimimus polyodon*, reconstructed and retrodeformed from CT scans. **A,** Right lateral view; **B,** dorsal view; **C,** ventral view. **Abbreviations: amcv,** anterior middle cerebral vein; **car,** internal carotid artery canal; **dp,** dural peak; **fl,** flocculus; **lab,** endosseous labyrinth; **pit,** pituitary fossa; **pmcv,** posterior middle cerebral vein; **ts,** transverse sinus; **V_{2-3},** maxillomandibular nerve canal; **VIII,** vestibulocochlear nerve canal; **IX_{stp},** stapedial branch of the glossopharyngeal nerve canal; **IX-XI,** shared canal for glossopharyngeal, vagus, and accessory nerves and accompanying vessels; **XII_{dor},** dorsal hypoglossal nerve canal; **XII_{ven},** ventral hypoglossal nerve canal; scale bar = 10 mm.

located ventral to the parietal and not in the parietal-frontal suture. The angle formed between the foramen magnum and the dural peak in lateral view is high (*ca.* 60º), like in *Struthiomimus* (Witmer & Ridgely, 2009).

The pituitary body is located ventrally in the endocast (Fig. 4A, 4C). Its posterior margin is located at the level of the root of the cranial nerve (CN) V. This margin is dorsoventrally oriented in lateral view. The anterior margin is situated at the level of the probable area of the root of the CN II, but this area of the braincase is incomplete. The anterior margin of the pituitary body is slightly posteroventrally oriented. The morphology of the body is slightly triangular in lateral view, but it could be deformed, and its anatomy could not be perfectly reconstructed due to the deformation. The pituitary body develops from the endocast just slightly anterior to the root of the CN V. It fits with the anteroposteriorly short braincase of *Pelecanimimus*. However, in other non-avian theropods, this is usually further anteriorly developed from the CN V, even in the ornithomimosaur *Struthiomimus* (Witmer & Ridgely, 2009). But in other maniraptoriforms, such as therizinosaurs (*Nothronychus* or *Falcarius*: Lautenschlager *et al.*, 2012), the pituitary body is also developed ventral to the hindbrain, just slightly anterior to the level of the CN V. In most posteroventral tips of the pituitary body, only the root of the internal carotid is developed (*e.g.,* Witmer & Ridgely, 2009). Still, it was not possible to see how to continue much internally in the pituitary fossa.

Cranial innervation and vascularization

Only the cranial nerves from the hindbrain region are identified (CN V to XII). The posterior middle cerebral veins originate from the dural peak in the hindbrain (Fig. 4A–4B). It is posteriorly oriented, and the veins get out of the braincase through the parietal-supraoccipital region occipitally. However, the foramina for the exits of these veins in the occipital view are not clearly observed in the braincase due to the disarticulation between the parietal and the supraoccipital. There is no evidence of a dorsal head vein, as in tyrannosauroids (Witmer & Ridgely, 2009). In the anterior point of the posterior middle cerebral vein, a transversal sinus is developed in the lateral surface of the endocast

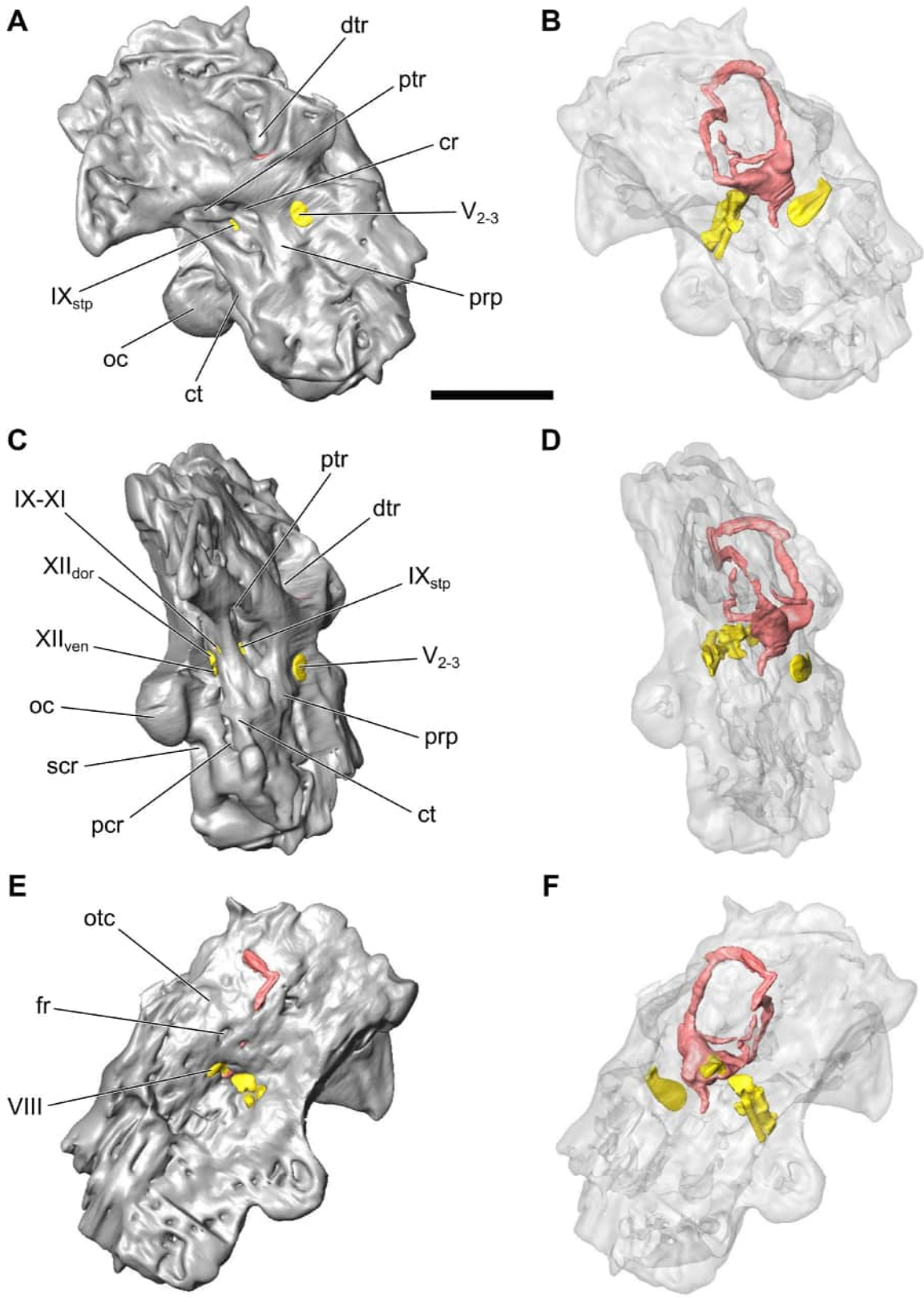

Figure 5. Digital reconstruction of the occipital region of the braincase of *Pelecanimimus polyodon* and distribution of cranial innervation and inner ear based on the CT scan. **A,** Right lateral view; **B,** right lateral view with semi-transparent braincase revealing internal endocast structures; **C,** right posteroventrolateral view; **D,** right posteroventrolateral view with semi-transparent braincase revealing internal endocast structures; **E,** medial view; **F,** medial view with semi-transparent braincase revealing internal endocast structures. **Abbreviations: cr,** columellar recess; **ct,** crista tuberalis; **dtr,** dorsal tympanic recess; **fr,** floccular recess; **oc,** occipital condyle; **otc,** otic cavity; **pcr,** paracondylar recess; **prp,** preotic pendant; **ptr,** posterior tympanic recess; **scr,** subcondylar recess; **V_{2-3},** maxillomandibular nerve foramen; **VIII,** vestibulocochlear nerve foramen; **IX_{stp},** stapedial branch foramen of the glossopharyngeal nerve; **IX-XI,** shared foramen for glossopharyngeal, vagus, and accessory nerves and accompanying vessels; **XII_{dor},** dorsal hypoglossal nerve foramen; **XII_{ven},** ventral hypoglossal nerve foramen; scale bar = 10 mm.

(Fig. 4A). It runs down to a dorsal point of the internal exit of the CN V. This would correspond to the anterior middle cerebral vein, as it is usual to radiate blood through the exit of this cranial nerve. This vein ends in the broken area corresponding to the contact between the missing laterosphenoid and the prootic. This might indicate that this vein exits through a foramen in the laterosphenoid, indicating a possible presence of an exit of the ophthalmic branch (V_1) (see below). The splitting of the trigeminal nerve into branches in separated passages is common in some groups of coelurosaurs (*e.g.,* Franzosa, 2004; Witmer & Ridgely, 2009; Lautenschlager *et al.*, 2012; Paulina-Carabajal *et al.*, 2021); thus, it might also be probable that it splits in Ornithomimosauria.

Right canals of the trigeminal (CN V), vestibulocochlear (CN VIII), glossopharyngeal (CN IX), vagus (CN X), accessory (CN XI) and hypoglossal (CN XII) nerves were partially or entirely identified. The external foramina of the facial nerve (CN VII) are identified in the external right side of the braincase of the specimen (Fig. 6), but its canals (hyomandibular and palatine branches, see below) are not preserved internally.

The CN V leaves the endocranial cavity through a single foramen in the medial wall of the braincase (Fig. 5). This foramen is anteroventrally located to the dorsal tympanic recess in the medial view of the braincase. Externally, the maxillo-mandibular branch ($V_{2,3}$) exits the braincase through an oval and wide foramen, slightly lateroposteriorly oriented. This broad foramen is completely enclosed in the prootic. Due to the laterosphenoid being completely missing in the specimen, it is not possible to identify if there is an ophthalmic branch (V_1) in *Pelecanimimus* or if all branches of CN V leave the braincase through the same foramen. However, as it was mentioned above, the possible identification of an anterior middle cerebral vein could indicate that the CN V of *Pelecanimimus* bifurcates into two branches.

The passage and the internal foramen for the CN VII are not observable in the CT scan. However, the external exit from the braincase is observable in the fossil (Fig. 6). This exit is formed by two small foramina, arranged dorsoventrally and posteriorly located to the foramen of the CN V in the prootic. This indicates that, in *Pelecanimimus,* the CN VII leaves the braincase by two branches: the palatine and the hyomandibular, like in other coelurosaurs, such as *Murusraptor* (Paulina-Carabajal & Currie, 2017) or *Shaochilong* (Brusatte *et al.*, 2010; considering a coelurosaur based on the phylogenetical hypothesis by Kellermann *et al.*, 2025). These foramina are posterior to the CN V, not internal to the same foramen as in tyrannosaurids (*e.g.,* Witmer & Ridgely, 2009; Paulina-Carabajal *et al.*, 2021).

The passage for the CN VIII was possible to identify in the CT scans partially (Fig. 4), as well as the foramen from where the nerve leaves the endocranial cavity through the vestibular eminence (Fig. 5E).

The passages for cranial nerves IX-XI leave the braincase together by a unique canal through the metotic foramen (Fig. 5C–5D). This foramen is located in the occipital region of the braincase, separated from the lateral wall by the *crista tuberalis*. This occipital exit is located dorsolaterally to the occipital condyle, enclosed between the exoccipital and the opisthotic, although the sutures are not well discernible. The

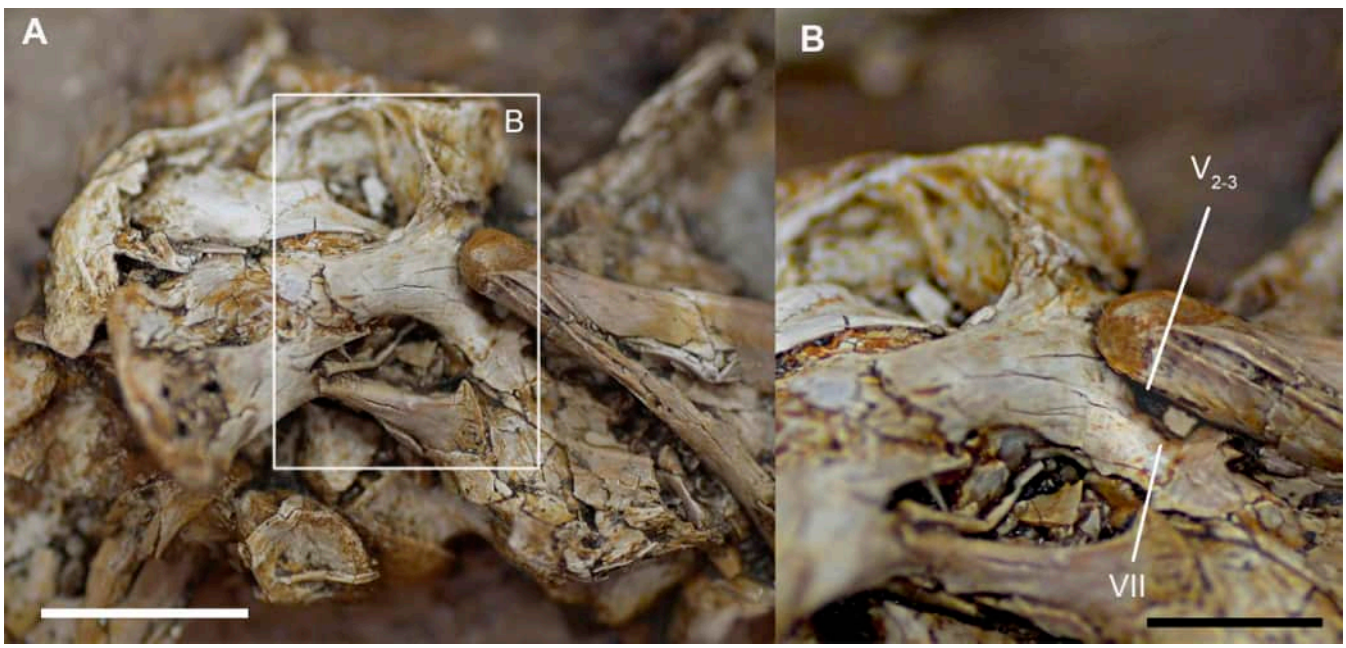

Figure 6. Right side of the occipital braincase of *Pelecanimimus polyodon* (MUPA-LH 7777). **A,** Lateral view of the complete occipital region of the braincase of the holotype; **B,** close-up of the region indicated in A, in a ventrolateral view, indicating the position of the foramina for the facial nerve (CN VII) respect to the maxillomandibular nerve (CN V_{2-3}) foramen. **Abbreviations: V_{2-3},** maxillomandibular nerve foramen; **VII,** facial nerve foramina; scale bars: A = 10 mm, B = 5 mm.

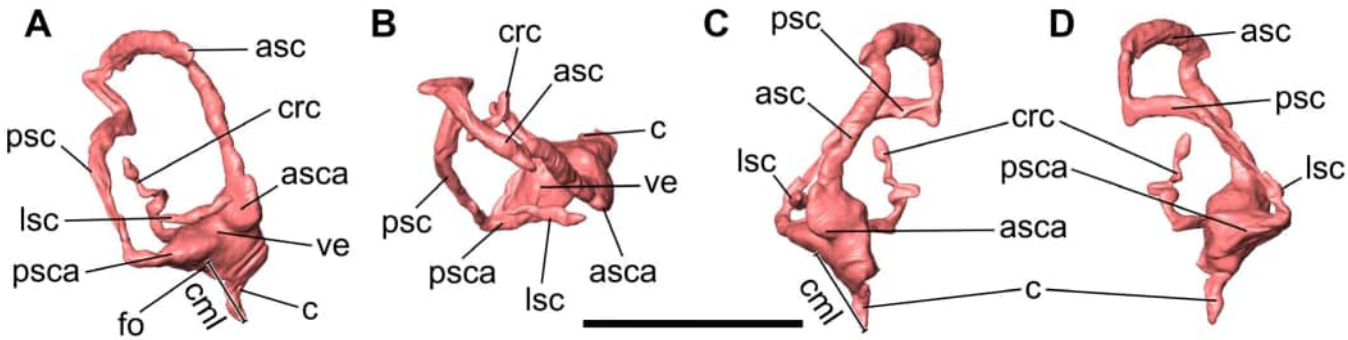

Figure 7. Right cast of the endosseous labyrinth of *Pelecanimimus polyodon*. **A,** Right lateral view; **B,** dorsal view; **C,** anterior view; **D,** posterior view. **Abbreviations: asc,** anterior semicircular canal; **asca,** ampulla of anterior semicircular canal; **c,** cochlear duct (= lagena); **cml,** cochlear duct maximum length; **crc,** crus communis; **fo,** fenestra ovalis; **lsc,** lateral semicircular canal; **psc,** posterior semicircular canal; **psca,** ampulla of posterior semicircular canal; **ve,** vestibule of inner ear; scale bar = 10 mm.

metotic foramen is oval and slightly dorsoventrally elongated and transversally broad, but not so much as the slit-like foramen in *Nothronychus, Erlikosaurus* and *Falcarius* (Lautenschlager *et al.*, 2012), or as broad as in *Daspletosaurus* (Paulina-Carabajal *et al.*, 2021). The same foramen for these nerves was probably the exit of the jugular vein. In addition to this common exit, the CN IX has an additional stapedial branch that leaves the endocranial cavity externally in the lateral wall of the braincase. It is posteroventral to the excavation of the columellar recess in the prootic and ventral to the posterior tympanic recess (Fig. 5). This stapedial branch of CN IX exit is also observed in *Murusraptor* (Paulina-Carabajal & Currie, 2017). In the endocranial surface of the braincase, there is an oval recess, more anteroposteriorly long than dorsoventrally broad, between the exits of the CN XII and the vestibular eminence, which corresponds to the *fovea ganglii vagoglossofaryngealis*. Through this recess, the CN IX-XI leaves the endocranial cavity by a single and transversally wide passage to their exits in the lateral wall and occipital region of the braincase (above mentioned).

The CN XII opens externally in the exoccipital, near the basis of the occipital condyle (Fig. 5C–5D). The external part of the channel is easily identified in the XY section of the CT scan. Still, it is difficult to maintain internal continuity due to the preservation state of the fossil. Two external foramina are identified for this nerve. The internal aperture is embedded into the context of the *fovea ganglii vagoglossofaryngealis*.

The CN XII of *Pelecanimimus* is represented by two canals, one more dorsally developed and thicker, and another ventral to the latter and thinner (Fig. 4A, 4C). The segmentation of the path of these two canals was challenging to follow, and thus, most of the paths were reconstructed. However, the foramina in the endocranial cavity and the occipital region of the braincase are well-defined. The CN XII leaves the endocranial cavity through two foramina posterior to the *fovea ganglii vagoglossofaryngealis* at the level of the medulla oblongata in the endocranial cast. Both are broad and well-developed foramina. Externally, the CN XII leaves the braincase through two foramina in the occipital region, dorsoventrally arranged around the lateral wall of the foramen magnum and slightly dorsolateral to the occipital condyle. The dorsal one is dorsoventrally elongated and larger than the ventral one, which is rounded (Fig. 5C–5D). Both are completely enclosed in the exoccipital.

Inner ear

The right inner ear was partially segmented. Since the deformation and preservation of the fossil, the complete osseous labyrinth was challenging to trace completely in the CT scan, and the segmented inner ear does not fully represent the original morphology. All the semicircular canals and the lagena (= cochlear duct) were digitally segmented from the CT scan, except part of the crus communis between the anterior semicircular canal (**asc**) and the posterior semicircular canal (**psc**), and the attachments between the lateral semicircular canal (**lsc**) and the ampullae.

The semicircular canals are generally slender and thin ($Ø_{asc}$ = 0.7 mm; $Ø_{psc}$ = 0.6 mm; $Ø_{lsc}$ = 0.6 mm) and, although the original thickness might have been affected by taphonomical compression, the anterior semicircular canal is thicker (Fig. 7). Despite the deformation, the anterior ampulla and the posterior ampulla are well-preserved, and the anterior semicircular canal and posterior semicircular canal are oriented nearly perpendicular to each other in dorsal view (Fig. 7B). However, the lateral semicircular canal orientation is not accurately interpreted because it is not entirely preserved and lacks the attachment areas with the ampullae. The anterior semicircular canal is the longest of the vestibular inner ear, and it has a complete inner length of 20.4 mm (Tab. 1). The posterior semicircular canal has approximately the half-length of the anterior semicircular canal (9.64 mm; Tab. 1). The segmented fragment of the lateral semicircular canal is 4.23 mm long (Tab. 1). In dorsal view, the semicircular canals form an angle of 77º. In the lateral view (Fig. 7A), the semicircular canals constitute an arc higher than wide,

Table 1. Segment and regional lengths obtained from the Skeletonization of the right inner ear of *Pelecanimimus polyodon*.

Segment of inner ear	Line number	Length (mm)	Total length (mm)	Total length (mm)
Anterior Semicircular Canal	0	20.3997	20.3997	20.40
Posterior Semicircular Canal	3	2.0607	9.637751	9.64
	4	0.680336		
	8	1.06592		
	9	1.26404		
	12	0.868309		
	14	0.468108		
	16	0.62003		
	18	0.503868		
	19	2.10644		
Lateral Semicircular Canal	20	4.22859	4.22859	4.23
Crus communis	11	6.90629	6.90629	6.91
Lagena	37	1.18305	4.00486	4.00
	40	0.62517		
	43	0.45714		
	45	1.7395		

and the dorsal region of the anterior semicircular canal arc is rounded like in *Struthiomimus* (see fig. 8Q–8T in Witmer & Ridgely, 2009) and birds (Walsh *et al.*, 2009). This morphology gives the vestibular system a more dorsoventrally rectangular outline in lateral view in *Pelecanimimus* and *Struthiomimus*, but unlike the triangular shape in other theropods (*e.g.,* Witmer & Ridgely, 2009; Cerroni & Paulina-Carabajal, 2019; Paulina-Carabajal & Nieto, 2019; Schade *et al.*, 2020; Paulina-Carabajal *et al.*, 2021), or the anteroposteriorly rectangular outline described in Therizinosauria (Lautenschlager *et al.*, 2012). The arc of the posterior semicircular canal has a semicircular outline and also a dorsal curvature, like *Struthiomimus* (Witmer & Ridgely, 2009) and Therizinosauria (Lautenschlager *et al.*, 2012), but also distinct to the more pointed dorsal surface in many other theropods (*e.g.,* Witmer & Ridgely, 2009; Cerroni & Paulina-Carabajal, 2019; Paulina-Carabajal & Nieto, 2019; Schade *et al.*, 2020; Paulina-Carabajal *et al.*, 2021). The anterior semicircular canal is dorsoventrally higher than the posterior semicircular canal and ascends above the dorsal point of the crus communis, like in most theropods (*e.g.,* Witmer & Ridgely, 2009; Lautenschlager *et al.*, 2012; Cerroni & Paulina-Carabajal, 2019; Paulina-Carabajal & Nieto, 2019; Paulina-Carabajal *et al.*, 2021). The morphology of the lateral semicircular canal is not possible to describe. The ampullae between the three canals are preserved, and they are laterally oriented and protrude laterally at the same level as the lateral semicircular canal. The anterior ampulla is as anteroposteriorly wide as dorsoventrally high, and the posterior ampulla is anteroposteriorly wider than dorsoventrally high, and they are gently developed relative to the thin semicircular canals. The crus communis is incomplete, and it is deformed; thus, the straight morphology is not observable, but it is vertically oriented as in most theropods (*e.g.,* Witmer & Ridgely, 2009; Lautenschlager *et al.*, 2012; Paulina-Carabajal *et al.*, 2021).

The lagena extends ventromedially from the vestibule. It is anteroposteriorly thick and sub-conical in its most dorsal region, but then it narrows ventrally. In this ventral region, the lagena is finger-shaped and tapers ventrally. Its most dorsal region is slightly anteriorly oriented in lateral view (Fig. 7A) and then it curves posteroventrally. In anterior view, its dorsal half curves slightly medially, parallel to the lateral surface of the endocast. The morphology of the lagena is not conservative in the three ornithomimosaurs with known inner ear. *Struthiomimus* has an anteroposteriorly thick lagena in its whole length, lacking the tapered finger-shape (Witmer & Ridgely, 2009), and *Tyrannomimus* has a full finger-shaped lagena. In this framework, *Pelecanimimus* has an intermediate morphology, with a dorsal thick lagena that turns finger shaped ventrally. However, the segmented morphology, at least in the case of *Pelecanimimus*, might be affected by the deformation of the fossil and not represent the accurate morphology. The lagena is 4 mm long (Tab. 1) from the fenestra ovalis. The lagena represents the 30% of the dorsoventral length of the inner ear. This proportion is similar to *Struthiomimus* (26%; Choiniere *et al.*, 2021), but the deinocheirid *Tyrannomimus* has a slightly longer lagena than *Pelecanimimus* (39%; Hattori *et al.*, 2023). That short lagena in some ornithomimosaurs is distinct from the elongated one in other coelurosaurs (Tab. 2) such as some tyrannosauroids (*Daspletosaurus,* 50%: Paulina-Carabajal *et al.*, 2021; *Alioramus,* 47%: Choiniere *et al.*, 2021; *Tyrannosaurus*, 42%: Witmer & Ridgely, 2009), therizinosaurs (*Erlikosaurus*, 45%: Lautenschlager *et al.*, 2012; *Falcarius*, 45%: Lautenschlager *et al.*, 2012), alvarezsaurids (*Shuvuuia,* 81%: Choiniere *et al.*, 2021; *Haplocheirus*, 44%: Choiniere *et al.*, 2021), or dromaeosaurids (*Dromaeosaurus,* 58%: Choiniere *et al.*, 2021; *Velociraptor,* 47%: Choiniere *et al.*, 2021). The fenestra ovalis was partially identified following the columellar canal within the braincase. However, this canal is filled with sediment and is not perfectly discernible in the CT scan. The fenestra ovalis is located in the region below the posterior ampulla, ventral to the lateral semicircular canal and facing slightly ventrolaterally (Fig. 7A).

DISCUSSION

The morphology of the cranial endocast recovered from *Pelecanimimus* has, in general, several features shared with other ornithomimosaurs like *Struthiomimus* (Witmer & Ridgely, 2009), and with some early-branching maniraptora (*e.g., Nothronychus, Falcarius*: Lautenschlager *et al.*, 2012) and derived maniraptora (*e.g., Deinonychus*: Witmer & Ridgely, 2009), or, even, with other non-maniraptoriform coelurosaurian theropods (Witmer & Ridgely, 2009). One of the

most recognisable features shared with other maniraptoriforms, such as *Struthiomimus* and *Deinonychus,* is the posteriorly positioned dural peak (Witmer & Ridgely, 2009). This dural peak is positioned a bit more anteriorly in other non-maniraptoriform coelurosaurs, such as *Tyrannosaurus* (Witmer & Ridgely, 2009) or *Daspletosaurus* (Paulina-Carabajal *et al.*, 2021). In ceratosaurs, basal tetanurans (*i.e.*, non-coelurosaurian tetanurans) and some early coelurosaurs, it is much more anteriorly localised. That is the case in *Majungasaurus*, *Allosaurus* (Witmer & Ridgely, 2009), *Carnotaurus* (Cerroni & Paulina-Carabajal, 2019), *Giganotosaurus* (Paulina-Carabajal & Nieto, 2019), *Acrocanthosaurus* (Franzosa & Rowe, 2005), or *Murusraptor* (Paulina-Carabajal & Currie, 2017). In Witmer and Ridgely (2009), two dural peaks, an anterior and a posterior, were identified in the endocranial cast of *Struthiomimus,* and the authors suggested that the anterior peak corresponds to the pineal apparatus. This anterior, or pineal peak of *Struthiomimus* has not been identified in *Pelecanimimus* because this structure should be more anterior in the endocast than the reconstructed region of *Pelecanimimus*. An anterior dural peak was also observed in some oviraptorosaurs (Balanoff *et al.*, 2014). However, Balanoff *et al.* (2014) proposed that the anterior protuberance would rather be a cast of the frontal-parietal suture due to its mediolateral expansion for *Conchoraptor* and *Incisivosaurus* (Oviraptorosauria). As derived ornithomimosaurs like *Struthiomimus* have paired frontals forming a double dome separated by a midline groove (Osmólska *et al.*, 1972; Kobayashi & Lü, 2003; Sues & Averianov, 2015), the hypothesis of Balanoff *et al.* (2014) fits for clarifying the occurrence of this anterior peak in *Struthiomimus* as it being a cast of the contact area between both paired frontals (see Dozo *et al.*, 2022 for more information). The presence or absence of this “anterior peak” in *Pelecanimimus* could clarify the identification of this structure in ornithomimosaurs and, hence, future studies of *Pelecanimimus* will be needed for further approaches.

The dural peak of *Pelecanimimus* has a reduced morphology. The sharp dural peak in early-branching coelurosaurs as *Tyrannosaurus* (Witmer & Ridgely, 2009) or *Daspletosaurus* (Paulina-Carabajal *et al.*, 2021) eases off in later nested clades from Coelurosauria, such as Ornithomimosauria (*e.g., Pelecanimimus*, *Struthiomimus*: Witmer & Ridgely, 2009) or Dromaeosauria (*e.g., Deinonychus*: Witmer & Ridgely, 2009). It nearly disappears in more-derived groups of Maniraptora, as Oviraptorosauria (*e.g., Conchoraptor, Incisivosaurus*: Balanoff *et al.*, 2014; *Citipati, Khaan*: Balanoff *et al.*, 2018) or early-branching Avialae (*Archaeopteryx*: Witmer & Ridgely, 2009; Balanoff *et al.*, 2014). The regular vascular imprints from the internal surface of the skull shown in other maniraptoriforms like the oviraptorid *Ingenia* or the ornithomimid ‘*Dromiceiomimus*’ (Osmólska, 2004) lead to the thought that the brain tightly fills the endocranial cavity in Maniraptoriforms, as shown for birds. Therefore, the reduced dural peak in *Pelecanimimus* comes from a tendency of reduction of this structure through the non-avian to avian brain evolution. This is a convergent feature shared with Oviraptorosauria (based on Balanoff *et al.*, 2014), and that might be caused by the reduction of the dura mater and venous sinuses due to the better-fitted endocranial cavity by the encephalon (based on Osmólska, 2004 and Dozo *et al.*, 2022).

Hearing

The length of the lagena is an indicator of the auditory capabilities of extinct animals (Witmer & Ridgely, 2009). The lagena of *Pelecanimimus* is short ventrally in comparison to the complete height of the osseous labyrinth, with a ratio of 0.30. This proportion is slightly greater than that of *Struthiomimus altus* (AMNH 5355), which has a ratio of 0.26 (see Tab. 2). Nevertheless, this proportion is even higher in deinocheirids such as *Tyrannomimus* (0.39; see Tab. 2). These short lagenae in some ornithomimosaurs contrast with the long lagenae in other coelurosaurs (Walsh *et al.*, 2009; Witmer & Ridgely, 2009; Lautenschlager *et al.*, 2012; Paulina-Carabajal *et al.*, 2021; see above). However, the ornithomimosaurian proportions are similar to that from some non-coelurosaurian theropods, such as *Allosaurus* or *Giganotosaurus* (Tab. 2), and some coelurosaurian ones, such as *Murusraptor* or *Nothronychus* (Tab. 2). Based on the estimation of the elongation of the lagena proposed by Choiniere *et al.* (2021), *Pelecanimimus* has a short qualitative elongation, established by the ratio between the length of the lagena and the height of the braincase (0.14; see Tab. 3). This elongation is also short for *Struthiomimus*, with a similar ratio to *Pelecanimimus* (0.15; see Tab. 3). Unfortunately, the elongation is not possible to be calculated in *Tyrannomimus*, due to the fragmentary nature of its braincase (Hattori *et al.*, 2023). This elongation is moderate in the therizinosaur *Erlikosaurus* (ratio = 0.26) and the tyrannosauroid *Alioramus* (ratio = 0.21) (Choiniere *et al.*, 2021; see Tab. 3). In the alvarezsauroid *Shuvuuia*, this ratio is significantly higher (0.64), representing that it is one of the coelurosaurs with a higher elongation (Choiniere *et al.*, 2021). Choiniere *et al.* (2021) correlated the relative elongation of the lagena with the diel activity pattern and foraging behaviours for 88 species of extant birds. Their results corroborate that greatly or moderately elongated lagenae are related to nocturnality patterns and auditory foraging behaviour (hunting abilities in low-light conditions), but not to facilitate intraspecific communication, since vocal learner birds have a shorter relative elongation. This moderate enlargement of the lagena appears in several non-avian dinosaur groups, such as the carnivorous tyrannosauroids or the great-sized herbivorous therizinosaurs, turning

Table 2. Lagena (= cochlear duct) length, complete endosseous labyrinth (= inner ear) height, and lagena length/labyrinth height ratio of avian and non-avian dinosaur species. The different species are ordered by taxonomical group. Measurements were taken following the method shown in Figure 3A.

Species	Group	Lagena length (mm)	Complete labyrinth height (mm)	Lagena / labyrinth ratio
Pelecanimimus polyodon	Ornithomimosauria	4.00	13.42	0.30
Struthiomimus altus	Ornithomimosauria	7.78	30.21	0.26
Tyrannomimus fukuiensis	Ornithomimosauria	7.88	20	0.39
Erlikosaurus andrewsi	Therizinosauria	12.28	24.81	0.49
Nothronychus mckinleyi	Therizinosauria	9.93	33.11	0.30
Falcarius utahensis	Therizinosauria	13.79	30.63	0.45
Falcarius utahensis	Therizinosauria	11.92	31.39	0.38
Alioramus altai	Tyrannosauroidea	17.87	38.25	0.47
Murusraptor barrosaensis	Tyrannosauroidea	9–11.5	37.3	0.24–0.31
Allosaurus fragilis	Allosauroidea	14.12	42.45	0.33
Giganotosaurus carolinii	Allosauroidea	14	48.5	0.29
Sinraptor dongi	Allosauroidea	18.56	40.72	0.46
Tyto alba	Strigiformes	12.4	13.49	0.92
Surnia ulula	Strigiformes	7.39	13.72	0.54
Podargus strigoides	Strisores	9.46	17.96	0.53
Steatornis caripensis	Strisores	6.84	11.82	0.58
Coturnix coturnix	Galliformes	4.31	7.54	0.57
Ara macao	Psittaciformes	6.74	12.26	0.55

into a high elongation in specialized alvarezsauroids like *Shuvuuia* (Choiniere *et al.*, 2021). Contrary to nocturnal activity and auditory foraging behaviour taxa, Ornithomimosauria and Oviraptorosauria have a short lagena in the results from the studies by Choiniere *et al.* (2021) (see Tab. 3). Based on the results here exposed, the short lagena of *Pelecanimimus* (Tab. 3) is consistent with the results put forth by Choiniere *et al.* (2021) for Ornithomimosauria. However, previous studies based on the scleral ring of *Pelecanimimus* (Calvo-Pérez *et al.*, 2023b) infer that this taxon was more active at night. The contradiction of these inferences regarding the diel activity pattern, which are based on both sensorial capabilities, could be explained by feeding behaviours. Ornithomimosaurs have been inferred to be herbivorous or omnivorous (*e.g.,* Zanno & Makovicky, 2011; Barrett, 2014). Therefore, *Pelecanimimus* might not be inferred to be a specialized nor highly active nocturnal hunter,

Table 3. Lagena length, braincase height, and lagena length/braincase height ratio of avian and non-avian dinosaur species. The different species are ordered by taxonomical group. Measurements were taken following the method shown in Figure 3. Qualitative elongation categories are assigned following Choiniere *et al.* (2021) (see suppl.).

Species	Group	Lagena length (mm)	Braincase height (mm)	Lagena length / braincase height ratio	Elongation (qualitative)
Pelecanimimus polyodon	Ornithomimosauria	4.00	28.38	0.14	Short
Struthiomimus altus	Ornithomimosauria	7.78	52.78	0.15	Short
Tyrannomimus fukuiensis	Ornithomimosauria	7.88	–	0.39	–
Khaan mckennai	Oviraptorosauria	7.35	42.47	0.17	Short
Erlikosaurus andrewsi	Therizinosauria	12.28	47.69	0.26	Moderate elongation
Shuuvuia deserti	Alvarezsauroidea	6.53	10.22	0.64	High elongation
Alioramus altai	Tyrannosauroidea	17.87	87	0.21	Moderate elongation
Sinraptor dongi	Allosauroidea	18.56	134	0.14	Short
Tyto alba	Strigiformes	12.4	26.37	0.47	High elongation
Surnia ulula	Strigiformes	7.39	26.42	0.28	Moderate elongation
Podargus strigoides	Strisores	9.46	27.77	0.34	Moderate elongation
Steatornis caripensis	Strisores	6.84	21.33	0.32	Moderate elongation
Coturnix coturnix	Galliformes	4.31	13.99	0.31	Limited elongation
Ara macao	Psittaciformes	6.74	31.37	0.21	Short

Table 4. Best frequency and high limit frequency ranges of hearing inferences for avian and non-avian dinosaur species. Calculations are made following the methodology of Gleich *et al.* (2005), based on body mass and basilar papilla length values.

Species	Group	Body mass (kg)	Basilar papilla length (mm)	Best frequency range (kHz)	High frequency range (kHz)
Pelecanimimus polyodon	Ornithomimosauria	11.5	2.67	1.76–2.96	4.29–6.50
Struthiomimus altus	Ornithomimosauria	276.2	5.19	1.28–1.58	3.39–3.95
Tyrannomimus fukuiensis	Ornithomimosauria	–	5.25	–	–
Archaeopteryx lithographica	Paraves	0.486	2.4	2.4–3.2	5.5–6.9
Dromaius novaehollandiae	Neornithes	60	5.5	~1.5	~3.8
Allosaurus fragilis	Allosauroidea	1400	8	0.78–1.08	2.48–3.04
Brachiosaurus (Giraffatitan) brancai	Titanosauriformes	75000	10.7	0.40–0.72	1.78–2.37

since its feeding behaviour would be more generalist and dependent on vision. However, further analyses are needed to evaluate these hypotheses.

Based on the correlation between the size of the lagena and the body mass (Gleich *et al.*, 2005), it is possible to estimate the sensitive frequencies of hearing for non-avian theropod dinosaurs. Zanno and Makovicky (2013) estimated a body mass of 11.5 kg for *Pelecanimimus* (see suppl. in Zanno & Makovicky, 2013). With a lagena length from the fenestra ovalis of 4 mm (Figs. 3A, 7A, 7C), a basilar papilla of 2.67 mm is calculated for *Pelecanimimus*. Following the extrapolations based on Gleich *et al.* (2005), the best frequency of hearing range for *Pelecanimimus* is 1.76–2.96 kHz (see Tab. 4). A linear regression is also established between both best frequencies of hearing, the one based on the body mass and the one based on the basilar papilla length, and the high-frequency limit of hearing (Gleich *et al.*, 2005). For *Pelecanimimus*, the high-frequency limit is below 6.50 kHz (within a range of 4.29–6.50 kHz; see Tab. 4). Compared with the estimations for large dinosaurs (*Allosaurus* and *Brachiosaurus* with the best frequency of hearing range of 0.8–1.08 kHz and 0.4–0.7 kHz, respectively, and a high-frequency limit of hearing below 3 kHz and 2.3 kHz, respectively; measurements obtained using the data in the supp. data from Gleich *et al.* (2005)), the estimations for *Pelecanimimus* agree with the hypothesis that 'small species with a short basilar papilla hear higher frequencies compared with larger species with a longer basilar papilla' (Gleich *et al.*, 2005). Within Ornithomimosauria, *Pelecanimimus* shows a wider range of frequencies than *Struthiomimus* (1.28–1.58 kHz; see Tab. 4). In the derived clades (Ornithomimidae and Deinocheiridae) of Ornithomimosauria, there is a trend towards gigantism (Zanno & Makovicky, 2013; Lee *et al.*, 2014; Cuesta *et al.*, 2021a; Chinzorig *et al.*, 2022). The derived ornithomimosaurid *Struthiomimus* achieved a body mass of 276 kg (see suppl. in Zanno & Makovicky, 2013), while the basal ornithomimosaur *Pelecanimimus* is among the smallest taxa in the group (11.5 kg; Zanno & Makovicky, 2013). Therefore, it is still in accordance with what Gleich *et al.* (2005) proposed, that *Pelecanimimus* has slightly better frequency of hearing even within Ornithomimosauria.

Equilibrium

The vestibular system is the part of the inner ear that controls the equilibrium and sense of balance, whose semicircular canals and ampullae manage the angular acceleration generated in the head (Witmer & Ridgely, 2009). Those canals are proportionally long and thin in *Pelecanimimus*, which match with other coelurosaurs (*e.g., Tyrannosaurus*, *Gorgosaurus*, *Struthiomimus*, *Deinonychus*, *Archaeopteryx*: Witmer & Ridgely, 2009; *Nothronychus*, *Falcarius*: Lautenschlager *et al.*, 2012; *Daspletosaurus*: Paulina-Carabajal *et al.*, 2021), that is associated with an agile and high-activity behaviour in Coelurosauria (Witmer & Ridgely, 2009). The elongation is especially noticeable in the anterior semicircular canal (asc), a feature that can be partially associated with bipedalism, as proposed by Sipla *et al.* (2004) and supported by Witmer and Ridgely (2009).

Together with the semicircular canals, the flocculus manages gaze stabilisation, which is done by stabilising retinal images when the head moves via the Vestibulo-Ocular Reflex and through compensatory head and neck movements (Dozo *et al.*, 2022). The presence of this structure in Theropoda and its relation with bipedalism remains unclear due to its absence in some bipedal ornithischians (Dozo *et al.*, 2022) and its presence in quadrupedal ornithischians like ankylosaurs (Miyashita *et al.*, 2011; Paulina-Carabajal *et al.* 2016, 2018) and stegosaurs (Galton, 1988, 2001). Unfortunately, the flocculus of *Pelecanimimus* was deformed, and its complete length is not accurately reconstructed. Nevertheless, a rounded-shaped dorsal region of the asc is shown in *Pelecanimimus*, *Struthiomimus* and other non-avian and avian coelurosaurs (*e.g.,* Witmer *et al.*, 2003; Walsh *et al.*, 2009; Lautenschlager *et al.*, 2012). Together with the enlargement of asc (see above), this could be related to the flocculus enlargement tendency of Maniraptoriforms, as shown in other taxa (*e.g., Struthiomimus*, *Deinonychus*; Witmer & Ridgely, 2009). However, according to some studies, relationships between the size of the flocculus and behavioural patterns in extinct vertebrates should be studied carefully (Walsh *et al.*, 2013; Ferreira-Cardoso *et al.*, 2017).

CONCLUSION

The data from the endocast of *Pelecanimimus polyodon* provides the best description in terms of palaeoneuroanatomy within Ornithomimosauria so far. The new data provided here help to broaden our knowledge of the morphology of the occipital region structures in the braincase of Ornithomimosauria and Coelurosauria, thus further clarifying our understanding of brain evolution in the avian lineage.

The endocranial traits in *Pelecanimimus* are similar to those shown in other ornithomimosaurs (*e.g., Struthiomimus*), and also congruent with evolutionary tendencies within Coelurosauria.

Pelecanimimus has a posteriorly located reduced dural peak, as shown in the nested groups of Maniraptoriforms. The inner ear holds a short lagena, which is a characteristic of *Struthiomimus*, making this a distinctive trait of Ornithomimosauria. This trait agrees with the hypothesis that proportionally shorter lagenae are shown in smaller species of dinosaurs, which is inversely correlated with the best hearing frequencies. In this fact, a most sensitive frequency of hearing of around 2.5 kHz and a high-frequency limit below 6.5 kHz are inferred for *Pelecanimimus*. These are more similar to that shown in modern and extinct birds than to the lower frequencies estimated for larger non-avian dinosaurs. The vestibular system is characterised by slender and elongated anterior and posterior semicircular canals, so agile and active behaviour is inferred for the species, as is also shown in other coelurosaurs. The elongation of asc and psc is associated with good control of the gaze stabilisation, and probably agrees with the floccular elongation tendency towards avian evolution.

The analysed traits and their implications are those expected for an early-branching maniraptoriform. Nevertheless, further palaeoneurological studies in *Pelecanimimus* and other ornithomimosaurs, both in description and inferences of sensorial capabilities, are needed to depict the neuroanatomical capacities of the group properly. Moreover, with all the current and future information about the palaeoneuroanatomy of theropods, future approaches to macroevolutionary quantitative analyses should be made for the complete clade Theropoda.

Supplementary information. This article has no additional data.

Author contributions. XCP and EC conceived the study. EC studied the anatomy of the fossil. XCP and EC studied the palaeoneuroanatomy. XCP segmented the palaeoneuroanatomical structures in the CT scans. XCP and EC wrote the manuscript.

Competing Interest. The authors declare no competing interests.

Funding. This study has been funded by the 2023 call of the grant program “Ayudas a Jóvenes Investigadores de la Sociedad Española de Paleontología” which was awarded by XCP.

Author details. **Xairo Calvo-Pérez**[1] & **Elena Cuesta**[2]. [1]Museu da Lourinhã, R. João Luís Moura, 95, 2530-158 Lourinhã, Portugal, xairocp@gmail.com; [2]SNSB-Bayerische Staatssammlung für Paläontologie und Geologie, Richard Wagner, 10, 80333, Munich, Germany, elena.cuestaf@gmail.com

Acknowledgements. We acknowledge M. Llandrés-Serrano (MUPA) and S. Langreo (former director of MUPA) for providing access to the holotype of *Pelecanimimus polyodon*. We also thank K. Miyata (FPDM) for access and assistance in conducting CT scan analyses. We thank M. Nicolas Nieto for his helpful remarks about palaeoneuroanatomy, and A. Paulina-Carabajal, B. von Backzo and P. Bona for their helpful guidance during “Anatomía neurocraneana de amniotas (no mamiferos) actuales y fósiles” course. Furthermore, we also would like to thank the Sociedad Española de Paleontología for providing funding. Finally, we thank Eduardo Puértolas Pascual and the anonymous reviewer for their critical comments, which have greatly helped to improve the manuscript.

REFERENCES

Balanoff, A. M., Bever, G. S., Rowe, T. B., & Norell, M. A. (2013). Evolutionary origins of the avian brain. *Nature*, *501*(7465), 93–96. doi: 10.1038/nature12424

Balanoff, A. M., Bever, G. S., & Norell, M. A. (2014). Reconsidering the avian nature of the oviraptorosaur brain (Dinosauria: theropoda). *PLoS ONE*, *9*(12), e113559. doi: 10.1371/journal.pone.0113559

Balanoff, A. M., Norell, M. A., Hogan, A. V., & Bever, G. S. (2018). The endocranial cavity of oviraptorosaur dinosaurs and the increasingly complex, deep history of the avian brain. *Brain Behavior and Evolution*, *91*(3), 125–135. doi: 10.1159/000488890

Barrett, P. M. (2005). The diet of ostrich dinosaurs (Theropoda: Ornithomimosauria). *Palaeontology*, *48*(2), 347–358. doi: 10.1111/j.1475-4983.2005.00448.x

Barrett, P. M. (2014). Paleobiology of herbivorous dinosaurs. *Annual Review of Earth and Planetary Sciences*, *42*, 207–230. doi: 10.1146/annurev-earth-042711-105515

Bever, G. S., Brusatte, S. L., Balanoff, A. M., & Norell, M. A. (2011). Variation, Variability, and the Origin of the Avian Endocranium: Insights from the Anatomy of *Alioramus altai* (Theropoda: Tyrannosauroidea). *PLoS ONE*, *6*(8), e23393. doi: 10.1371/journal.pone.0023393

Benson, R. B., Starmer-Jones, E., Close, R. A., & Walsh, S. A. (2017). Comparative analysis of vestibular ecomorphology in birds. *Journal of Anatomy*, *231*(6), 990–1018. doi: 10.1111/joa.12726

Brusatte, S. L., Chure, D. J., Benson, R. B., & Xu, X. (2010). The osteology of *Shaochilong maortuensis*, a carcharodontosaurid (Dinosauria: Theropoda) from the Late Cretaceous of Asia. *Zootaxa*, *2334,* 1–46. doi: 10.11646/zootaxa.2334.1.1

Calvo-Pérez, X., Vidal, D., & Cuesta, E. (2022). Peer into the *Pelecanimimus* eye: sclerotal ring reconstruction of an Early Cretaceous ornithomimosaur from Spain. *Abstract book of the XIX Annual Conference of the European Association of Vertebrate Palaeontologists* (pp. 29–30). Benevento/Pietraroja.

Calvo-Pérez, X., Vidal, D., Sanz, J. L., & Cuesta, E. (2023a). “Walking in the shadows” with *Pelecanimimus*: Were

early-branched ornithomimosaurs nocturnal? *Abstracts book of XXI EJIP / 6th IMERP* (pp. 29). Lourinhã.

Calvo-Pérez, X., Vidal, D., Sanz, J. L., & Cuesta, E. (2023b). "Dancing in the Moonlight" with *Pelecanimimus*: Unraveling the visual capabilities of the Early Cretaceous ornithomimosaur from Las Hoyas. *Libro de Resúmenes de las XXXVIII Jornadas SEP* (pp. 134). Valencia.

Cerroni, M. A., & Paulina-Carabajal, A. (2019). Novel information on the endocranial morphology of the abelisaurid theropod *Carnotaurus sastrei*. *Comptes Rendus Palevol*, *18*(8), 985–995. doi: 10.1016/j.crpv.2019.09.005

Chinzorig, T., Cullen, T., Phillips, G., Rolke, R., & Zanno, L. E. (2022). Large-bodied ornithomimosaurs inhabited Appalachia during the Late Cretaceous of North America. *PLOS One*, *17*(10), e0266648. doi: 10.1371/journal.pone.0266648

Choiniere, J. N., Neenan, J. M., Schmitz, L., Ford, D. P., Chapelle, K. E. J., Balanoff, A. M., Sipla, J. S., Georgi, J. A., Walsh, S. A., Norell, M. A., Xu, X., Clark, J. M., & Benson, R. B. J. (2021). Evolution of vision and hearing modalities in theropod dinosaurs. *Science*, *372*(6542), 610–613. doi: 10.1126/science.abe7941

Christiansen, P., & Fariña, R. A. (2004). Mass prediction in theropod dinosaurs. *Historical biology*, *16*(2–4), 85–92. doi: 10.1080/08912960412331284313

Cuesta, E., Ortega, F., & Sanz, J. L. (2018a). The skull of *Pelecanimimus polyodon* (Theropoda, Lower Cretaceous, Spain): comparative approach to Asian Ornithomimosauria. *Abstract book of the 6th International Symposium of IGCP 608: Asia-Pacific Cretaceous Ecosystems* (pp. 78–80). Khon Kaen.

Cuesta, E., Ortega, F., & Sanz, J. L. (2018b). Scanning the skull of *Pelecanimimus polyodon* (Ornithomimosauria, Early Cretaceous, Spain): Osteological Approach. *Abstract book of the XVI Annual Meeting of the European Association of Vertebrate Palaeontology* (pp. 54). Caparica.

Cuesta, E., Vidal, D., Ortega, F., Shibata, M., & Sanz, J. L. (2021a). *Pelecanimimus* (Theropoda: Ornithomimosauria) postcranial anatomy and the evolution of the specialized manus in Ornithomimosaurs and sternum in maniraptoriforms. *Zoological Journal of the Linnean Society*, *194*(2), 553–591. doi: 10.1093/zoolinnean/zlab013

Cuesta, E., Vidal, D., Ortega, F., & Sanz, J. L. (2021b). *Pelecanimimus* (Theropoda, Ornithomimosauria) skull: from laminated limestone to 3D reconstruction and retrodeformation. *Abstract book of the XVIII annual conference of the European Association of Vertebrate Paleontologists* (pp. 63). Online.

Dozo, M. T., Paulina-Carabajal, A., Macrini, T. E., & Walsh, S. (2022). *Paleoneurology of amniotes*. Springer. doi: 10.1007/978-3-031-13983-3

Ferreira-Cardoso, S., Araújo, R., Martins, N. E., Martins, G. G., Walsh, S., Martins, R. M. S., Kardjilov, N., Manke, I., Hilger, A., & Castanhinha, R. (2017). Floccular fossa size is not a reliable proxy of ecology and behaviour in vertebrates. *Scientific Reports*, *7*(1), 2005. doi: 10.1038/s41598-017-01981-0

Franzosa, J. W. (2004). *Evolution of the brain in Theropoda (Dinosauria)*. (PhD Thesis, The University of Texas, Austin). Available at https://repositories.lib.utexas.edu/handle/2152/1145

Franzosa, J., & Rowe, T. (2005). Cranial endocast of the Cretaceous theropod dinosaur Acrocanthosaurus atokensis. *Journal of Vertebrate Paleontology*, *25*(4), 859–864. doi: 10.1671/0272-4634(2005)025

Galton, P. M. (1988). Skull bones and endocranial casts of stegosaurian dinosaur *Kentrosaurus* Hennig, 1915 from Upper Jurassic of Tanzania, East Africa. *Geologica et Palaeontologica*, *22*, 123–143.

Galton, P. M. (2001). Endocranial casts of the plated dinosaur *Stegosaurus* (Upper Jurassic, western USA): a complete undistorted cast and the original specimens of Othniel Charles Marsh. In K. Carpenter (Ed.), *The armored dinosaurs* (pp. 103–129). Indiana University Press.

Gleich, O., Dooling, R. J., & Manley, G. A. (2005). Audiogram, body mass, and basilar papilla length: correlations in birds and predictions for extinct archosaurs. *The Science of Nature*, *92*(12), 595–598. doi: 10.1007/s00114-005-0050-5

Hattori, S., Shibata, M., Kawabe, S., Imai, T., Nishi, H., & Azuma, Y. (2023). New theropod dinosaur from the Lower Cretaceous of Japan provides critical implications for the early evolution of ornithomimosaurs. *Scientific Reports*, *13*(1), 13842. doi: 10.1038/s41598-023-40804-3

Kellermann, M., Cuesta, E., & Rauhut, O. W. (2025). Re-evaluation of the Bahariya Formation carcharodontosaurid (Dinosauria: Theropoda) and its implications for allosauroid phylogeny. *PLOS One*, *20*(1), e0311096. doi: 10.1371/journal.pone.0311096

Kobayashi, Y., & Lü, J. C. (2003). A new ornithomimid dinosaur with gregarious habits from the Late Cretaceous of China. *Acta Palaeontologica Polonica, 48*(2), 235–259.

Kundrát, M. (2007). Avian-like attributes of a virtual brain model of the oviraptorid theropod *Conchoraptor gracilis*. *The Science of Nature*, *94*(6), 499–504. doi: 10.1007/s00114-007-0219-1

Lautenschlager, S., Rayfield, E. J., Altangerel, P., Zanno, L. E., & Witmer, L. M. (2012). The endocranial anatomy of therizinosauria and its implications for sensory and cognitive function. *PLOS One*, *7*(12), e52289. doi: 10.1371/journal.pone.0052289

Lee, Y. N., Barsbold, R., Currie, P. J., Kobayashi, Y., Lee, H. J., Godefroit, P., Escuillié, F., & Chinzorig, T. (2014). Resolving the long-standing enigmas of a giant ornithomimosaur Deinocheirus mirificus. *Nature*, *515*(7526), 257–260. doi: 10.1038/nature13874

Makovicky, P. J., Kobayashi, Y., & Currie, P. J. (2004). Ornithomimosauria. *The Dinosauria*, 137–150.

Makovicky, P. J., & Norell, M. (1998). A partial ornithomimid braincase from Ukhaa Tolgod (Upper Cretaceous, Mongolia). *American Museum Novitates, 3247*, 1–16.

McKeown, M., Brusatte, S. L., Williamson, T. E., Schwab, J. A., Carr, T. D., Butler, I. B., Muir, A., Schroeder, K., Espy, M. A., Hunter, J. F., Losko, A. S., Nelson, R. O., Gautier, D. C., & Vogel, S. C. (2020). Neurosensory and Sinus Evolution as Tyrannosauroid Dinosaurs Developed Giant Size: Insight from the Endocranial Anatomy of *Bistahieversor sealeyi*. *The Anatomical Record*, *303*(4), 1043–1059. doi: 10.1002/ar.24374

Miyashita, T., Arbour, V. M., Witmer, L. M., & Currie, P. J. (2011). The internal cranial morphology of an armoured dinosaur Euoplocephalus corroborated by X-ray computed tomographic reconstruction. *Journal of Anatomy*, *219*(6), 661–675. doi: 10.1111/j.1469-7580.2011.01427.x

Osmólska, H. (2004). Evidence on relation of brain to endocranial cavity in oviraptorid dinosaurs. *Acta Palaeontologica Polonica*, *49*(2), 321–324.

Osmólska, H., Roniewicz, E., & Barsbold, R. (1972). A new dinosaur, *Gallimimus bullatus* n. gen., n. sp. (Ornithomimidae) from the Upper Cretaceous of Mongolia. *Palaeontologia Polonica*, *27*, 103–143.

Paulina-Carabajal, A. P., & Canale, J. I. (2010). Cranial endocast of the carcharodontosaurid theropod *Giganotosaurus carolinii* Coria Salgado, 1995. *Neues Jahrbuch Für Geologie Und Paläontologie - Abhandlungen*, *258*(2), 249–256. doi: 10.1127/0077-7749/2010/0104

Paulina-Carabajal, A., & Currie, P. J. (2012). New information on the braincase and endocast of *Sinraptor dongi* (Theropoda: Allosauroidea): Ethmoidal region, endocranial anatomy and pneumaticity. *Vertebrata Palasiatica*, *50*, 85–101.

Paulina-Carabajal, A., & Currie, P. J. (2017). The braincase of the theropod dinosaur *Murusraptor*: osteology, neuroanatomy and comments on the paleobiological implications of certain endocranial features. *Ameghiniana*, *54*(5), 617. doi: 10.5710/amgh.25.03.2017.3062

Paulina-Carabajal, A., Currie, P. J., Dudgeon, T. W., Larsson, H. C., & Miyashita, T. (2021). Two braincases of *Daspletosaurus* (Theropoda: Tyrannosauridae): anatomy and comparison. *Canadian Journal of Earth Sciences*, *58*(9), 885–910. doi: 10.1139/cjes-2020-0185

Paulina-Carabajal, A., & Filippi, L. (2018). Neuroanatomy of the abelisaurid theropod *Viavenator*: The most complete reconstruction of a cranial endocast and inner ear for a South American representative of the clade. *Cretaceous Research*, *83*, 84–94. doi: 10.1016/j.cretres.2017.06.013

Paulina-Carabajal, A., Lee, Y., & Jacobs, L. L. (2016). Endocranial Morphology of the Primitive Nodosaurid Dinosaur *Pawpawsaurus campbelli* from the Early Cretaceous of North America. *PLOS One*, *11*(3), e0150845. doi: 10.1371/journal.pone.0150845

Paulina-Carabajal, A., Lee, Y. N., Kobayashi, Y., Lee, H. J., & Currie, P. J. (2018). Neuroanatomy of the ankylosaurid dinosaurs *Tarchia teresae* and *Talarurus plicatospineus* from the Upper Cretaceous of Mongolia, with comments on endocranial variability among ankylosaurs. *Palaeogeography, Palaeoclimatology, Palaeoecology*, *494*, 135–146. doi: 10.1016/j.palaeo.2017.11.030

Paulina-Carabajal, A., & Nieto, M. N. (2019). Brief Comment on the Brain and Inner Ear of *Giganotosaurus carolinii* (Dinosauria: Theropoda) Based on CT Scans. *Ameghiniana*, *57*(1), 58–62. doi: 10.5710/amgh.25.10.2019.3237

Pérez-Moreno, B. P., Sanz, J. L., Buscalioni, A. D., Moratalla, J. J., Ortega, F., & Rasskin-Gutman, D. (1994). A unique multitoothed ornithomimosaur dinosaur from the Lower Cretaceous of Spain. *Nature*, *370*(6488), 363–367. doi: 10.1038/370363a0

Sanders, R. K., & Smith, D. K. (2005). The endocranium of the theropod dinosaur *Ceratosaurus* studied with computed tomography. *Acta Palaeontologica Polonica*, *50*(3), 601–616.

Schade, M., Rauhut, O. W. M., & Evers, S. W. (2020). Neuroanatomy of the spinosaurid *Irritator challengeri* (Dinosauria: Theropoda) indicates potential adaptations for piscivory. *Scientific Reports*, *10*(1), 9259. doi: 10.1038/s41598-020-66261-w

Sipla, J., Georgi, J., & Forster, C. (2004). The Semicircular Canals of Dinosaurs: Tracking major transitions in locomotion. *Journal of Vertebrate Paleontology, 24*(S3)*: Abstracts of papers from the 64th annual meeting of the Society of Vertebrate Paleontology* (pp. 113A). Denver.

Sues, H., & Averianov, A. (2015). Ornithomimidae (Dinosauria: Theropoda) from the Bissekty Formation (Upper Cretaceous: Turonian) of Uzbekistan. *Cretaceous Research, 57*, 90–110. doi: 10.1016/j.cretres.2015.07.012

Walsh, S. A., Barrett, P. M., Milner, A. C., Manley, G., & Witmer, L. M. (2009). Inner ear anatomy is a proxy for deducing auditory capability and behaviour in reptiles and birds. *Proceedings of the Royal Society B Biological Sciences*, *276*(1660), 1355–1360. doi: 10.1098/rspb.2008.1390

Walsh, S. A., Iwaniuk, A. N., Knoll, M. A., Bourdon, E., Barrett, P. M., Milner, A. C., Nudds, R. L., Abel, R. L., & Sterpaio, P. D. (2013). Avian cerebellar floccular fossa size is not a proxy for flying ability in birds. *PLOS One*, *8*(6), e67176. doi: 10.1371/journal.pone.0067176

Witmer, L. M., Chatterjee, S., Franzosa, J., & Rowe, T. (2003). Neuroanatomy of flying reptiles and implications for flight, posture and behaviour. *Nature*, *425*(6961), 950–953. doi: 10.1038/nature02048

Witmer, L. M. (1997). Craniofacial air sinus systems. In P. J. Currie, & K. Padian, (Eds.), *Encyclopedia of dinosaurs* (pp. 151–159). Academic Press.

Witmer, L. M., & Ridgely, R. C. (2009). New Insights Into the Brain, Braincase, and Ear Region of *Tyrannosaurs* (Dinosauria, Theropoda), with Implications for Sensory Organization and Behavior. *The Anatomical Record*, *292*(9), 1266–1296. doi: 10.1002/ar.20983

Zanno, L. E., & Makovicky, P. J. (2011). Herbivorous ecomorphology and specialization patterns in theropod dinosaur evolution. *Proceedings of the National Academy of Sciences*, *108*(1), 232–237. doi: 10.1073/pnas.1011924108

Zanno, L. E., & Makovicky, P. J. (2013). No evidence for directional evolution of body mass in herbivorous theropod dinosaurs. *Proceedings of the Royal Society B Biological Sciences*, *280*(1751), 20122526. doi: 10.1098/rspb.2012.2526

Zelenitsky, D. K., Therrien, F., & Kobayashi, Y. (2008). Olfactory acuity in theropods: palaeobiological and evolutionary implications. *Proceedings of the Royal Society B Biological Sciences*, *276*(1657), 667–673. doi: 10.1098/rspb.2008.1075

Zelenitsky, D. K., Therrien, F., Ridgely, R. C., McGee, A. R., & Witmer, L. M. (2011). Evolution of olfaction in non-avian theropod dinosaurs and birds. *Proceedings of the Royal Society B Biological Sciences*, *278*(1725), 3625–3634. doi: 10.1098/rspb.2011.0238